Mesoscopic resist processing simulation in optical lithography

T. Schnattinger, E. Bär, A. Erdmann
Fraunhofer Institute of Integrated Systems and Device Technology (IISB)
Schottkystrasse 10, 91058 Erlangen, Germany
Email: thomas.schnattinger@iisb.fraunhofer.de

***Abstract*— Line-edge roughness (LER) control and minimization are among the critical issues for the further advancements in EUV and optical lithography. For the simulation of LER, discrete and stochastic models are required. This paper presents an improved stochastic exposure simulation model. It is proven that it is not necessary to take the Poisson distribution of the photon statistics into account. Mesoscopic exposure and post exposure bake models are compared with continuous, deterministic models in terms of obtained CD values, convergence behavior, and required computing time. The results obtained with both methods show a very good agreement.**

I. Introduction

Due to the increasing importance of line-edge roughness (LER), its modeling is an important factor for the future benefit of resist processing simulation tools. Experimentally, the inherent stochastic fluctuations during the exposure and post exposure bake (PEB) process have been identified as important contributors to LER.

Based on previous work on stochastic exposure [1] and reaction/diffusion [2] simulations, the exposure model is simplified by proving that the Poisson distribution of the photons can be ignored in a stochastic exposure simulation. In addition, mesoscopic (i.e. probabilistic and discrete) exposure and PEB simulations are for the first time compared with established continuous and deterministic simulations.

For the image formation and continuous resist processing simulations, the IISB lithography simulator Dr.LiTHO [3] is used. A positive tone chemically amplified photoresist is simulated. The parameters haven been chosen close to previously calibrated values. Key parameters of the lithography simulation are listed in Table I. In all simulations, an equidistant discretisation in x, y, and z direction is used. The diffusion processes where assumed to be Fickian.

II. Exposure

During exposure of the resist, incident light converts some photoacid generator (PAG) molecules to acid. In continuous, deterministic models, the relative acid concentration after exposure at position ($A(\vec{x})$), where $\vec{x}$ is the position in the 3D space, depends on the resist sensitivity, described by Dill's C parameter, and the locally absorbed dose $I(\vec{x})$:

$$A(\vec{x}) = 1 - e^{-CI(\vec{x})} \tag{1}$$

For our mesoscopic simulations, the expected value of the local dose $I(\vec{x})$ is obtained by continuous, deterministic bulk image simulations. To incorporate the stochastic fluctuations during exposure, previous simulation approaches by Yuan and Neureuther [1] include two sources of noise. First, the dose fluctuation in the average area (M) occupied by a PAG is simulated. Based on the expected value, the probability that actually k photons incur ($p_k(IM/\hbar\omega)$) is described by the Poisson distribution given in Equation 2:

$$p_k(IM/\hbar\omega) = \frac{(IM/\hbar\omega)^k}{k!} e^{-IM/\hbar\omega} \tag{2}$$

$\hbar\omega$ is the energy per photon. Second, the generation of acid molecules is simulated by using the previously obtained dose density and reinterpreting Equation 1 for each PAG as the probability that it is transformed.

Below, a new, much simpler but mathematically equivalent, stochastic exposure model is presented. Provided that a PAG is not yet converted, each photon incurring in the area M associated with a PAG has an equal probability $r \leq 1$ to generate an acid. In the following this area is reduced by a factor of $m = 1/r$ and accordingly the probability that a photon incurring in this reduced area ($c = M/m$, called effective cross section) converts the PAG becomes unity. Since r denotes the probability that a single photon does convert the PAG, $(1 - r)^k$ is the probability that k photons cause no conversion of the PAG. The probability that a PAG is not

TABLE I
Key lithography parameters used in the simulations

Parameter	Value
Exposure wavelength	193 nm
Numerical aperture	0.9
Resist dimensions (x,y,z)	(200, 200, 200) nm
Dill A	0 μm^{-1}
Dill B	0.5 μm^{-1}
Dill C	0.36 cm^2/mJ
Post exposure bake time	90 s
Relative base concentration	0.1
Acid diffusion length	23 nm
Base diffusion length	100 nm

converted to acid is then given by

$$q(I,m) = \sum_{k=0}^{\inf} p_k(IM/\hbar\omega)(1-r)^k = \sum_{k=0}^{\inf} p_k(Imc/\hbar\omega)(1-\frac{1}{m})^k \quad (3)$$

Using Equation 2, this can be rewritten as

$$q(I,m) = \sum_{k=0}^{\inf} \frac{(Imc/\hbar\omega)^k}{k!} e^{-Imc/\hbar\omega}(1-\frac{1}{m})^k \quad (4)$$

$$= e^{-Imc/\hbar\omega} \sum_{k=0}^{\inf} \frac{(Imc/\hbar\omega - Ic/\hbar\omega)^k}{k!}$$

$$= e^{-Ic/\hbar\omega} e^{-Ic(m-1)/\hbar\omega} \sum_{k=0}^{\inf} \frac{(I(mc-1)/\hbar\omega)^k}{k!}$$

Now the Taylor series of the exponential function is substituted, leading to

$$q(I,m) = e^{-cI/\hbar\omega} e^{-Ic(m-1)/\hbar\omega} e^{Ic(m-1)/\hbar\omega} = e^{-cI/\hbar\omega} \quad (5)$$

Equations 3 to 5 prove that changing the size of the area associated with a single PAG – provided that it is greater or equal than the effective cross section – and adopting the probability that a single photons causes a PAG conversion does not affect the resulting probability distribution of generated acids. The term $e^{-cI/\hbar\omega}$ is the Poisson probability that no photon occurs in the area of the effective cross section (compare Equation 2) and therefore the probability that a PAG survives, in accordance with Equation 1. The resist sensitivity C is now described in terms of the effective cross section c of the PAGs, which is also a intuitive interpretation for the parameter resist sensitivity.

As explained in the following, it is also intuitively clear that the probability that a single PAG is converted to acid is just equal to the relative acid concentration obtained at the corresponding position with continuous, deterministic exposure simulation models. All PAG conversions to acid are stochastically independent of each other since they depend only on the locally incident number of photons. However, in both previously published models about stochastic exposure simulation [1], [4], there has been no awareness that it is not necessary to model the Poisson distribution of the photons (i.e. photon shot noise) for a correct stochastic exposure simulation. This made the exposure models not only more complex than necessary, but in particular less computationally efficient. Without the explicit modeling of photon shot noise, a speed up of the exposure simulation times by a factor of over 3 has been achieved. Acid concentration distributions after the exposure process obtained with the continuous, deterministic and the mesoscopic exposure models are shown in Figure 1(a) and 1(b), respectively.

III. Post exposure bake

In the subsequent PEB simulation, three chemical species are accounted for: dissolution inhibitor, base, and the acid generated during exposure. During this process step, neutralization of acid and base, diffusion of acid and base, and acid catalyzed deprotection of inhibitor are simulated.

In the continuous model, the chemical species are represented as normalized concentrations, with values ranging from 0 to 1 in each cell. The post exposure bake time is divided into fixed time-steps and the reaction and diffusion processes are simulated iteratively [3]. The number of steps the PEB time is divided into has a considerable effect on the numerical accuracy (see Figure 3(a)) and the required computing time (see Figure 3(b)). For the given simulation parameters (see Table I), about 1000 time steps are necessary to achieve a sufficient convergence.

For the mesoscopic PEB simulation, an algorithm previously employed for the reaction/diffusion process simulation of individual molecules in biological cells [2] is used. This event-based approach provides a rigorously coupled simulation of all reaction and diffusion events. The chemical species are represented as individual molecules in each resist cell. An event is then either the diffusion of an acid or base molecule to a neighboring cell, or the reaction of acid with base or inhibitor within a single cell.

IV. Comparison of continuous and mesoscopic models

For the first time, mesoscopic exposure and PEB simulations are compared with deterministic, continuous models. Due to the nondeterministic properties of the mesoscopic models, a quantitative comparison, especially of the intermediate results like acid concentration after exposure, is not straightforward.

When comparing the obtained acid concentration after the exposure step, the standing wave patterns visible in the continuous model (Figure 1(a)) are still recognizable in the results obtained with the mesoscopic simulations (Figure 1(b)), despite significant stochastic fluctuations. To allow a comparison of the resulting resist profiles, the development rates are computed based on the obtained inhibitor concentrations after the PEB. The subsequent development process has been simulated with a Fast Marching algorithm [5]. The resulting resist profiles indicate also the consistency of both methods. The low contrast standing wave patterns obtained with the continuous model (Figure 2(a)) are also recognizable in the profile obtained with the mesoscopic simulations (Figure 2(b)).

The CD values obtained with the continuous model (using at least 1000 time steps) and the average CD values of the mesoscopic model differ by about 1 nm (see Figure 3(a)) and are thus lower than the differences obtained when comparing numerically different continuous models [5]. With both methods, a spatial resolution of 150 gridpoints in each direction (corresponding to a cell edge length of 1.3 nm) provides a sufficient convergence.

In terms of required computing time, the mesoscopic model falls behind the continuous model (see Figure 3(b)). A major

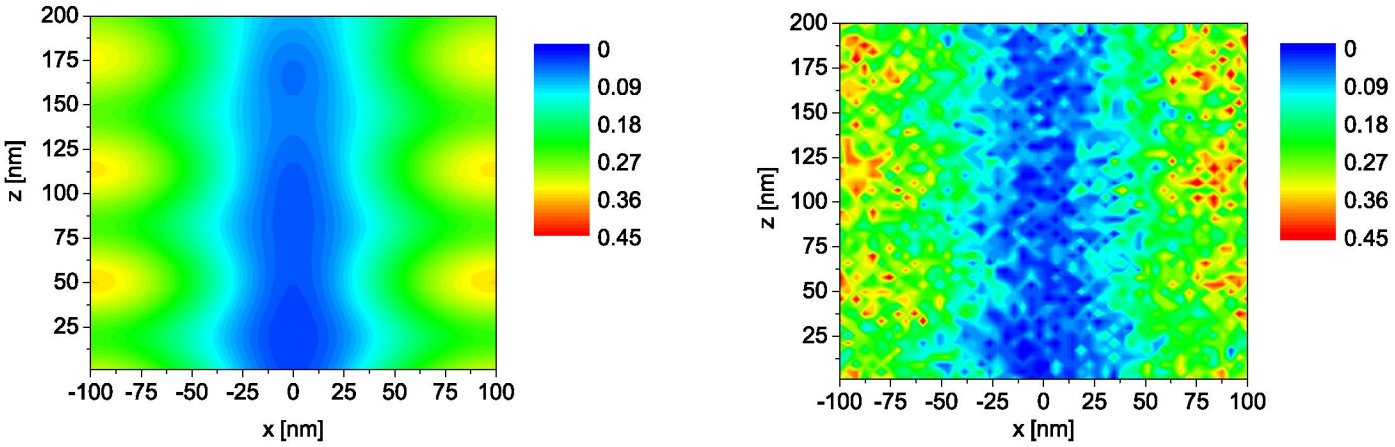

(a) (b)

Fig. 1. Acid concentration distribution after the exposure process simulated with a continuous, deterministic (a) and mesoscopic (b) exposure model. A vertical cut through a 3D simulation of a resist line is shown.

reason for the speed advantage of the continuous, deterministic algorithms is that they can exploit the invariance (homogeneity) of the resist properties in one space dimension. In fact, we compare a two-dimensional continuous, deterministic simulation with a 3D mesoscopic simulation. For the sole purpose of CD simulations, also the mesoscopic model could be reduced to two dimensions.

The computing time required for the mesoscopic model depends also on the absolute acid and inhibitor concentration values (less particles mean a lower computing time) and diffusion constants (lower diffusion lengths lead to fewer diffusion events that have to be simulated). Since the computing time required for the continuous model does not depend on any of those factors, the differences in the required computing time can be considerably different for other simulation settings.

V. Line-edge roughness dependencies

Several process and material parameters are experimentally known to affect the resulting LER values. Among them are the aerial image quality (contrast and log slope), the base (quencher) concentration and the exposure dose, or the acid and base diffusion lengths [6], [7], [8]. In this work, LER is quantified as three times the standard deviation of the actual line-edge from a linear fit (3σ method). Figure 4 shows the simulated impact of the aerial image quality on the resulting LER in terms of varying numerical aperture (Figure 4(a)) and projector defocus (Figure 4(b)). The simulated results confirm the experimental measurements that a worse aerial image quality (caused here by an increased defocus or decreased numerical aperture) increases the resulting LER of the resist profile. It has to be taken into account that a change in the numerical aperture or projector defocus does not only change the roughness but also the average CD of the resulting profile. Due to the usage of a continuous, deterministic development simulation algorithm, the impact of the polymer size and shapes as well as the influence of dissolution inhomogenities are not accounted for in this work.

VI. Conclusions

The new mesoscopic algorithms show a very good matching with the established continuous approaches. Their benefit is the inclusion of the stochastic nature of the exposure and PEB process, that are major contributors to LER [4]. The drawback of mesoscopic models is the higher computing time required. The new stochastic exposure simulation approach provides a considerably faster method. For full process simulations, however, most of the computing time ($> 75\%$) is required for the PEB simulation. The mesoscopic PEB simulation requires a computing time around three to four times larger than for continuous models with 1000 PEB steps (see Figure 3(b)). One focus of future work will thus be the performance optimization of mesoscopic PEB simulations. Additional future work will be the combination with mesoscopic development models to include the additional contributions of the resist structure and development process to the resulting LER.

References

[1] L. Yuan and A. Neureuther, Proc. SPIE 5376, 212 (2004).
[2] J. Elf, A. Doncic, M. Ehrenberg, Proc. SPIE 5110, 114 (2003).
[3] Dr.LiTHO, development and research lithography simulation toolkit, Fraunhofer IISB, 2006.
[4] R. Brainard, P. Trefonas, J. Lammers, C. Cutler, J. Mackevich, A. Trefonas, S. Robertson, Proc. SPIE 5374, 74 (2004).
[5] T. Schnattinger, E. Bär, Proc SISPAD 2005, 215 (2005).
[6] D. Steenwinckel, J. Lammers, T. Koehler, R. Brainard, P. Trefonas, J. Vac. Sci. Technol. B24(1) (2006)
[7] M. Ercken, L. Leunissen, I. Pollentier, G. Patsis, V. Constantoudis, E. Gogolides, Proc. SPIE 5375, 266 (2004)
[8] M. Ryoo, S. Shirayone, H. Oizumi, N. Matsuzawa, S. Irie, E. Yano, S. Okazaki, Proc. SPIE 4345, 903 (2001)

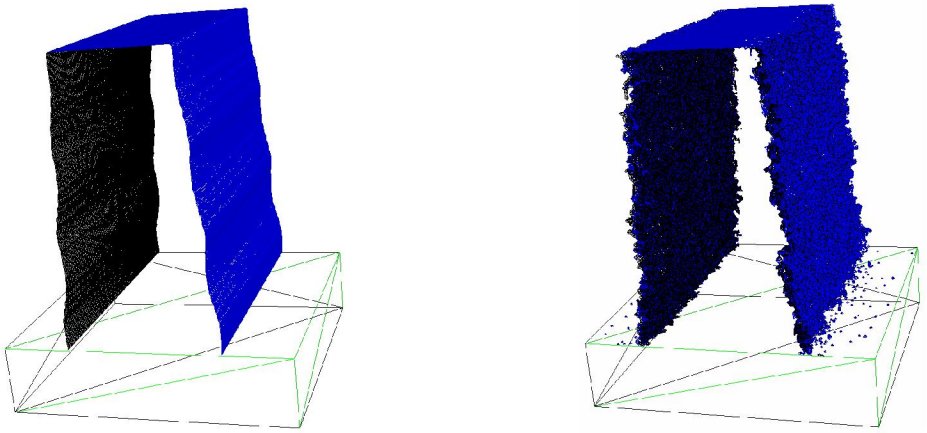

(a) (b)

Fig. 2. Resist profiles obtained with continuous, deterministic (a) and mesoscopic (b) exposure and post exposure bake simulation. A discretisation of 150 gridpoints in x, y, and z direction was used.

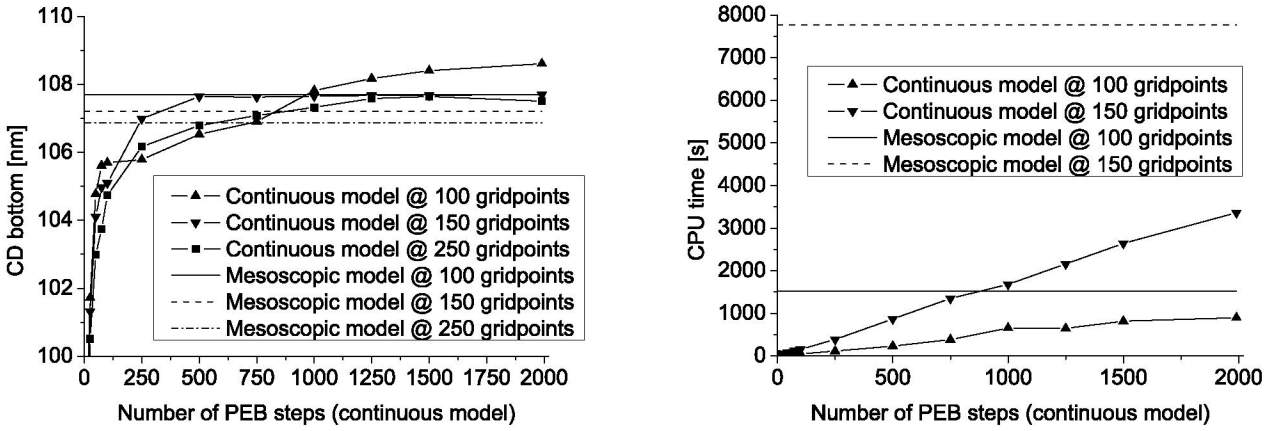

(a) (b)

Fig. 3. Comparison of the continuous, deterministic model in dependence of the number of post exposure bake steps with the mesoscopic model in terms of obtained CD values (a) and required computing times (b).

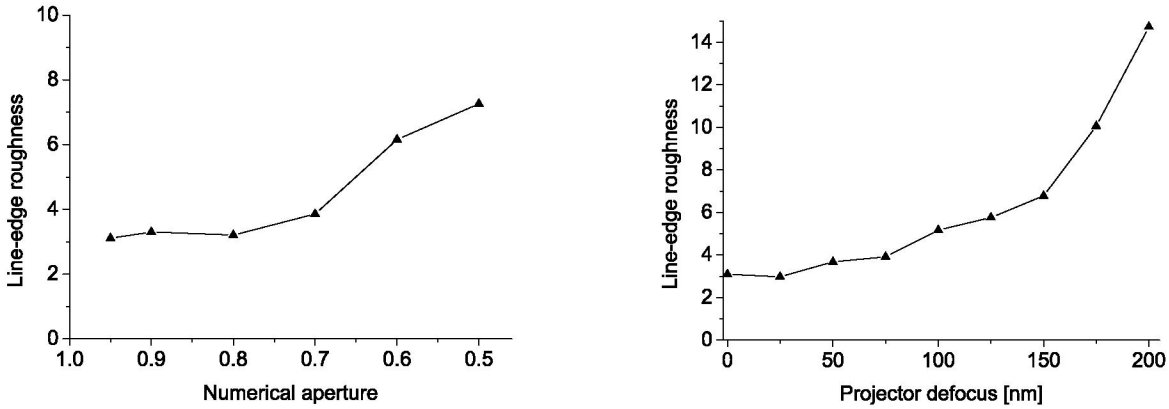

(a) (b)

Fig. 4. Line-edge roughness dependence on the numerical aperture (a) and the projector defocus (b).

